Relativistic and non-relativistic orbits

ME 275: Advanced Dynamics
Final Project
Dennis Wai
May 2nd, 2012

Introduction

Developed in the 1860s, Newton's Theory of Gravitation provided an easy explanation for many of the phenomenon observed in planetary motion. Grounded in the fact that gravity is a force of attraction between two massive objects, Newtonian gravity is not perfect and fails to account for anomalies found from observations in the orbits of planets like Mercury. In the 1900s, Einstein's general theory of relativity provided a geometric basis for gravitation as well as a satisfying explanation for the anomalies that Newtonian gravity could not address.

In this project, differences and similarities of orbits formed between the Earth and Sun is explored in both the non-relativistic Newtonian case and the relativistic general relativity case. Finally, Mercury's orbit in space will also be investigated with respect to both models of gravitation.

Situation

In the analysis to follow, this paper considers the motion of a body of mass m around a non-moving object of mass M. The coordinates of the mass m are parametrized by a set of spherical polar coordinates, R, ϕ, and θ.

In the non-relativistic case (Newtonian case), the motion of mass m is under the influence of the conservative gravitational potential field. In the relativistic case (Einstein case), the motion of mass m obeys space-time's geodesics with respect to the Schwarzschild metric:

$$ds_s^2 = c^2\left(1 - \frac{2MG}{Rc^2}\right)(dt)^2 - \left(1 - \frac{2MG}{Rc^2}\right)^{-1}(dR)^2 - R^2((d\phi)^2 + sin^2(\phi)(d\theta)^2) \quad (1)$$

Earth - Sun orbit

In the following section, the paper will use the Earth-Sun system as an example to demonstrate similarities and differences between the two gravitation model. In the context of this paper, $M_{sun} = 1.99 \times 10^{30} kg$, $G = 6.67 \times 10^{-11} m^3 kg^{-1} s^{-2}$, and $c = 3.00 \times 10^8 m/s$. G is the universal gravitational constant and c is the speed of light.

Non-relativistic Orbits

To generate phase portraits for the non-relativistic case, the Lagrangian for the system must be expressed:

$$L = \frac{m}{2}(\dot{R}^2 + (R\dot{\phi})^2 + R^2 sin^2(\phi)\dot{\theta}^2) + \frac{GMm}{R} \tag{2}$$

From the Lagrangian, a set of three equations of motion are obtained. For the scope of this paper, of particular interest are the ones concerning R and θ:

$$\frac{d^2R}{dt^2} = R\left(\frac{d\phi}{dt}\right)^2 + Rsin^2(\phi)\left(\frac{d\theta}{dt}\right)^2 - \frac{GM}{R^2} \tag{3}$$

$$R^2 sin^2(\phi)\frac{d\theta}{dt} = p_\theta \tag{4}$$

The integral of motion can be used in conjunction with the chain rule to rewrite our differential equation such that we have an expression of $R(\theta)$ instead of $R(t)$. The relationship between the two is as shown:

$$\frac{dR}{dt} = \frac{dR}{d\theta}\frac{d\theta}{dt}$$

$$= \frac{dR}{d\theta}\frac{p_\theta}{R^2} \tag{5}$$

$$\frac{d^2R}{dt^2} = \frac{d^2R}{d\theta^2}\left(\frac{d\theta}{dt}\right)^2 + \frac{dR}{d\theta}\frac{d^2\theta}{dt^2}$$

$$= \frac{d^2R}{d\theta^2}\frac{p_\theta^2}{R^4} - 2\frac{p_\theta}{R^3}\frac{dR}{d\theta} \tag{6}$$

From the homework, it was determined that ϕ and $\dot{\phi}$ are equal to $\frac{\pi}{2}$ and 0, respectively. Combining that fact with the results above, the differential equations collapse to:

$$\frac{d^2R}{d\theta^2} = R + \frac{2}{R}\left(\frac{dR}{d\theta}\right)^2 - \frac{GMR^2}{p_\theta^2} \tag{7}$$

For large values of R (i.e. as we go farther away from the mass M), the difference between the

non-relativistic case and relativistic case diminishes. As a result, the coordinate transform $R = \frac{1}{u}$ is used to provide an alternative form to (??):

$$\frac{d^2u}{d\theta^2} = \frac{MG}{p_\theta^2} - u \tag{8}$$

Using the non-dimensionalized parameter $u = \frac{GM}{p_\theta^2}x$, the equation simplifies further to:

$$\frac{d^2x}{d\theta^2} = 1 - x \tag{9}$$

The phase portrait for this differential equation is shown in Fig. ??:

Discussion

After applying a coordinate transformation, the behavior of the Earth-Sun system under the Newtonian case is brought into full view. As seen from the phase portrait, Fig. ??, the four types of orbit behavior - circular, elliptical, parabolic, and hyperbolic - are stable (i.e. form closed orbits). According to [?], the circular orbit is signified by the center red dot and the ellipses adjacent to it, counting from inside to outside, represent elliptical, parabolic and hyperbolic orbits. Therefore, under the non-relativistic case there is no limit to the distance between the Earth and Sun because all of the orbits are stable.
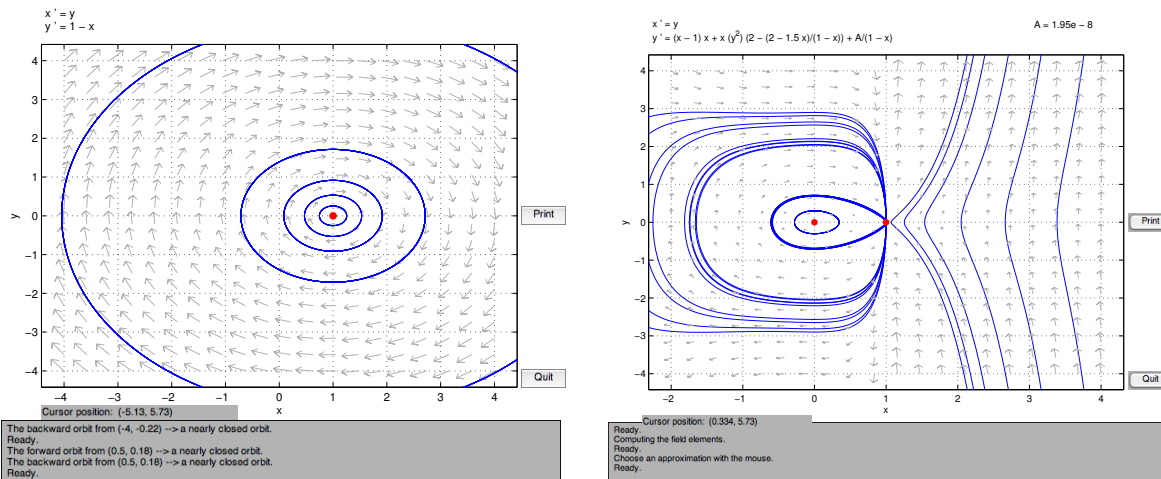
(a) Figure for non-relativistic orbits. Observe that orbits are closed and stable for all values of x

(b) Figure for relativistic orbits. Observe that orbits beyond x = 1(i.e when $R_s = R$) is senseless because those orbits lie within the event horizon

Figure 1: Phase portraits for both the non-relativistic and relativistic case for the Sun-Earth system. The x axis is x whereas the y axis is $\frac{dx}{d\theta}$

3

Relativistic Orbits

Since relativistic orbits are based on the geodesics of space-time, the Schwarzschild line metric, Eq. (1), is used to derive the equations of motion. After setting the initial conditions $\phi = \frac{\pi}{2}$ and $\dot{\phi} = 0$ and performing some algebra, the equations of relevance are:

$$\ddot{R} = \left(1 - \frac{R_s}{R}\right)\frac{p_\theta^2}{R^3} + \left(1 - \frac{R_s}{R}\right)^{-1}\frac{R_s}{2R^2}\left(\dot{R}^2 - \frac{p_t^2}{c^2}\right) \tag{10}$$

$$p_t = c^2\left(1 - \frac{R_s}{R}\right)\dot{t}$$

$$p_\theta = R^2\dot{\theta} \tag{11}$$

where $R_s = \frac{2MG}{c^2}$ is the Schwarzschild radius, which is the critical radius that an object of mass M must exceed in order to not become a black hole. Similar to above, R must be a function of θ so the chain rule and the p_θ relation is invoked again to arrive at this expression:

$$\frac{d^2R}{d\theta^2} = \left(1 - \frac{R_s}{R}\right)R + \frac{1}{R}\left(\frac{4\frac{R}{R_s} - 3}{2\frac{R}{R_s} - 2}\right)\left(\frac{dR}{d\theta}\right)^2 - \left(1 - \frac{R_s}{R}\right)^{-1}\frac{R_s p_t^2 R^2}{c^2 p_\theta^2} \tag{12}$$

Applying the coordinate transform, $R = \frac{1}{u}$ and then non-dimensionalizing it with the parameter $u = \frac{x}{R_s}$, the equation transforms to:

$$\frac{d^2u}{d\theta^2} = (R_s u - 1)u + \frac{1}{u}\left(\frac{du}{d\theta}\right)^2\left(2 - \frac{2 - 1.5R_s u}{1 - R_s u}\right) + \frac{R_s p_t^2}{2(1 - R_s u)p_\theta^2 c^2} \tag{13}$$

$$\frac{d^2x}{d\theta^2} = x(x - 1) + x\left(\frac{dx}{d\theta}\right)^2\left(2 - \frac{2 - 1.5x}{1 - x}\right) + \frac{1}{2(1 - x)}\left(\frac{p_t R_s}{p_\theta c}\right)^2 \tag{14}$$

The phase portrait associated with this differential equation is shown in Fig. **??**. The parameter $A = \left(\frac{p_t R_s}{p_\theta c}\right)^2 = 1.95 \times 10^{-8}$ was previously calculated in homework and represents a constant specific to the planet of interest.

Discussion

The phase portrait for relativistic orbit is dramatically different from that of the non-relativistic case. The phase portrait can be split into two halves along the vertical at $x = 1$. The left half represents viable orbits for the Earth-Sun system and varying orbit types, such as the circular, elliptical, parabolic and hyperbolic variety The circular orbit is the equilibrium point found at (0,0) (or in other words, at $R = \infty$). As the orbits move radially outward, the orbits become more hyperbolic. The right half, however, represents values of $x > 1$ (when $R \leq R_s$). In other words, mass m passed the event horizon of the black hole and is now stuck. As an aside, although calculations were done based on the Earth-Sun system, the orbits depicted in Fig. **??** are unobtainable in the physical world because this analysis ignores the geometries of the celestial bodies (i.e. $R_s << R_{sun}$).

4

Mercury's orbit

Now the focus will be placed on Mercury and its orbit as predicted by the non-relativistic and relativistic model. For the scope of this paper, $M_{Mercury} = 3.3 \times 10^{23} kg$ and its orbital period is 87.96 days.

Non-relativistic Orbit

From Eq.(**??**), the non-relativistic motions of Mercury can be determined and reconstructed. The following dimensionless parameters are used

$$\tau = \frac{G^2 M_{Mercury}^2}{p_\theta^3} t \quad and \quad R = \frac{p_\theta^2}{GM} x \tag{15}$$

to arrive at the following set of non-relativistic, nondimensionalized equations of motions for Mercury.

$$\frac{d^2 x}{d\tau^2} = \frac{1}{x^3} - \frac{1}{x^2} \tag{16}$$

$$\frac{d\theta}{d\tau} = \frac{1}{x^2} \tag{17}$$
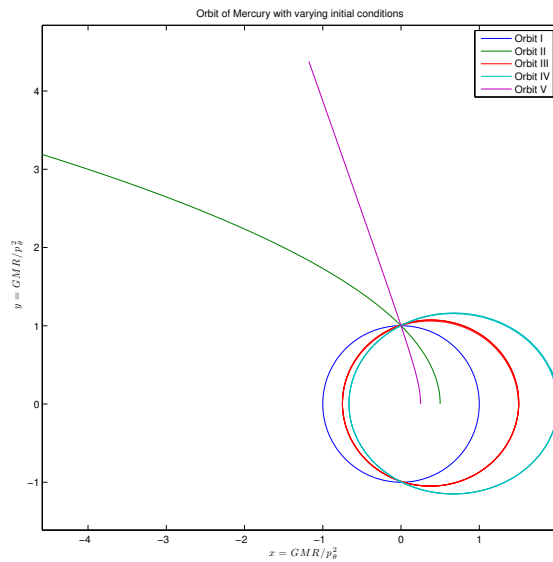
Figure 2: All of the possible orbits suggested by the phase portrait Fig.(**??**), superimposed upon one another in space. The Roman numbering is related to which orbit was chosen (see Fig. (**??**)) The origin is located at (0,0)

.

Relativistic Orbit

To examine the Mercury's physical orbits in the Einstein case, we start with Eq.(**??**) and choose the following to be the appropriate dimensionless parameters

$$\tau = t\frac{p_\theta}{R^2} \quad and \quad x = \frac{R}{R_s} \tag{18}$$

and after some algebra, the following set of differential equations describe the relativistic motion of Mercury.

$$\frac{d^2x}{d\tau^2} = (x-1) + \frac{1}{2x(x-1)}\left(\frac{dx}{d\tau}\right)^2 + \frac{Ax^3}{(x-1)} \tag{19}$$

$$\frac{d\theta}{d\tau} = 1 \tag{20}$$

where $A = \frac{p_t^2 R_s^2}{2p_\theta^2 c^2} = 5.15 \times 10^{-8}$ for Mercury.
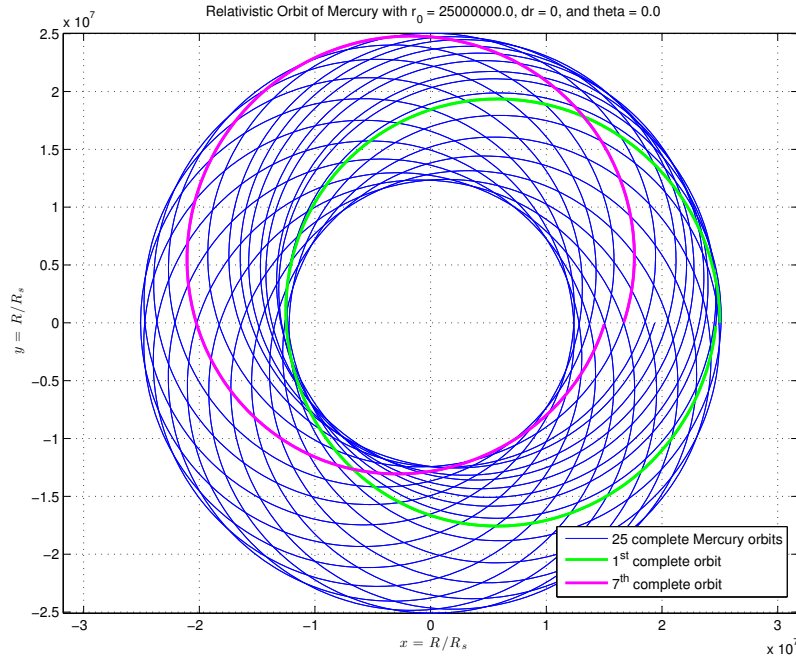
Figure 3: Mercury's physical orbit numerically integrated by ODE45 for a long time interval. Unique to the relativistic model, the precession observed here is also physically present in Mercury's orbit

Discussion

Comparing the phase portrait between the non-relativistic and relativistic case, it's easy to observe that there are distinctive from one another. Most noticeably, the relativistic phase portrait has extremely distorted orbits near $x = 1$ to reflect the event horizon found accompanying black holes. Taking the aforementioned differential equations, ODE45 was used to recreate the physical orbits of Mercury under the non-relativistic and relativistic model. In the non-relativistic case, the orbits found are beautiful. As the initial conditions vary, the body's orbit will evolve from a perfectly circular orbit to an ellipse to a parabolic orbit and then finally to a hyperbolic orbit. This is clearly demonstrated in Fig.(**??**) and Fig.(**??**)

The orbits recreated from the relativistic phase portrait are just as interesting. The additional A term in the equation hints that the relativistic equations are system-specific. A prime example of this is that the circular orbit equilibrium point is located a great distance away from the origin to reflect the actual average distance between the Sun and Mercury. Another interesting thing to observe is that, unique to the relativistic model, is precession in Mercury's orbit. This is most prominently featured in Fig.(**??**) where the first and seventh revolution of Mercury is highlighted in green and magenta, respectively, to demonstrate this phenomenon. Finally, the relativistic model also indicates presence of black holes and as shown in Fig.(**??**), orbits that collides with the event horizon will cause nonsensical, non-plottable data to be calculated.

References

[1] Oliver O'Reilly, *Intermediate Dynamics for Engineers: A United Treatment of Newton-Euler and Lagrangian Mechanics* Cambridge University Press, Cambridge 2nd Edition 2008

Figure 4: Phase portrait with several chosen trajectories alongside its physical orbits in space
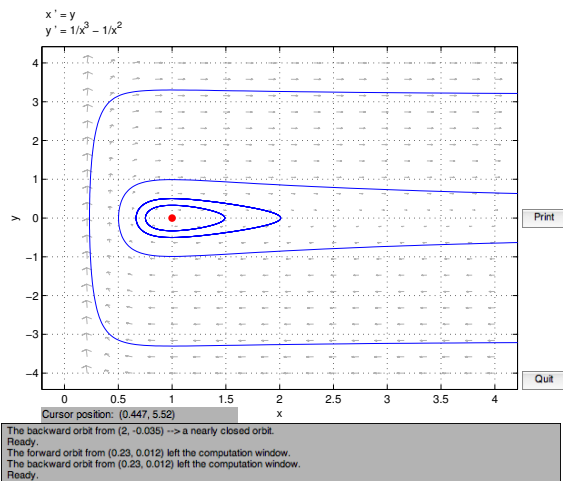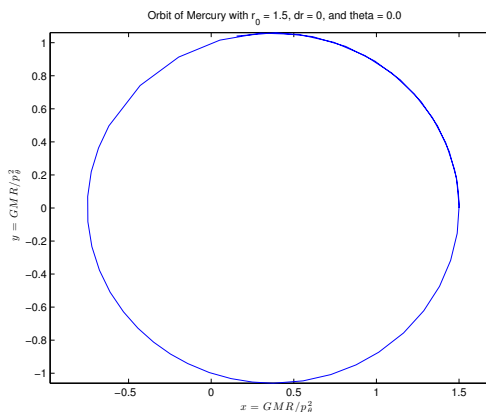

(a) Phase portrait generated by Eq.(**??**). Going radially outward, the chosen orbits are: I) the equilibrium point $(1,0)$; II) the orbit at $(.5,0)$; III) the orbit at $(1.5,0)$; IV) the orbit at $(2,0)$; and V) the orbit at $(.25,0)$ The x axis is the nondimensionalized parameter x and the y axis is $\frac{dx}{d\tau}$.
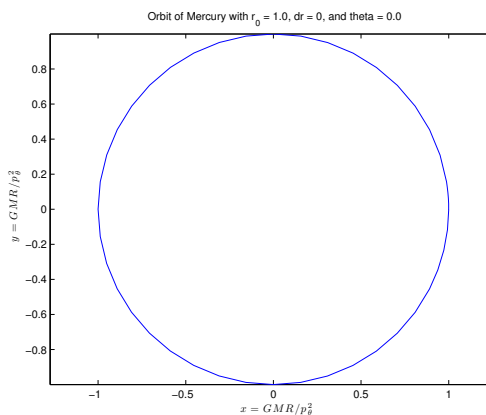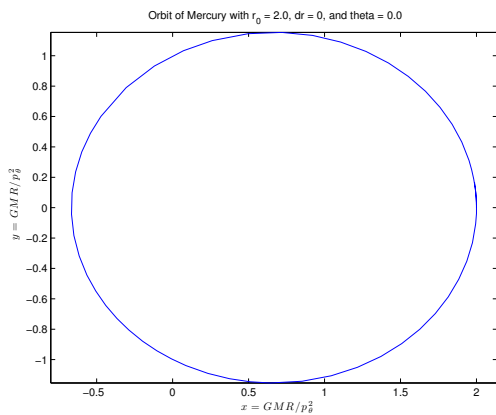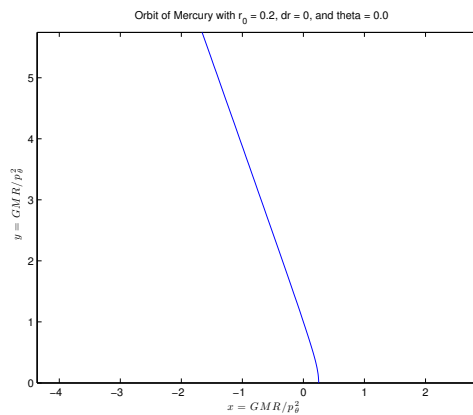

(b) I Circular orbit
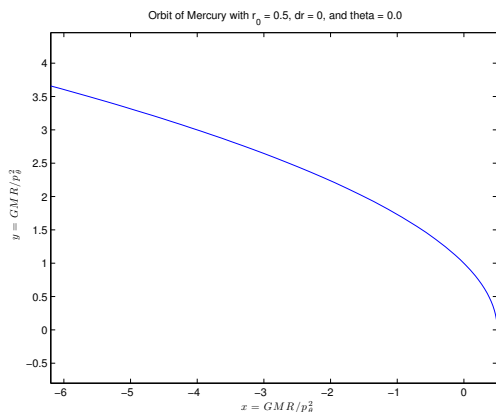
(c) II Parabolic orbit
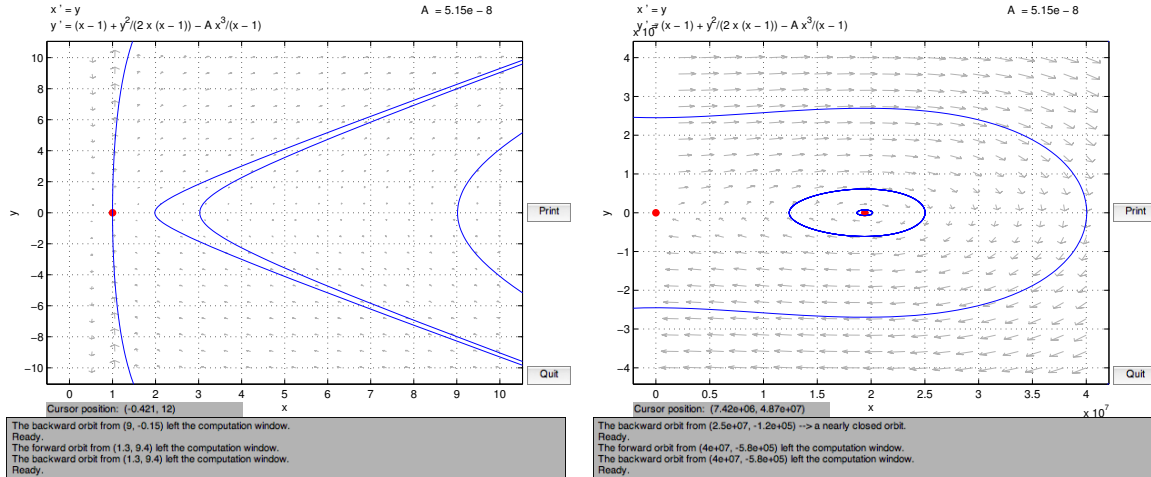

(d) III Elliptical orbit
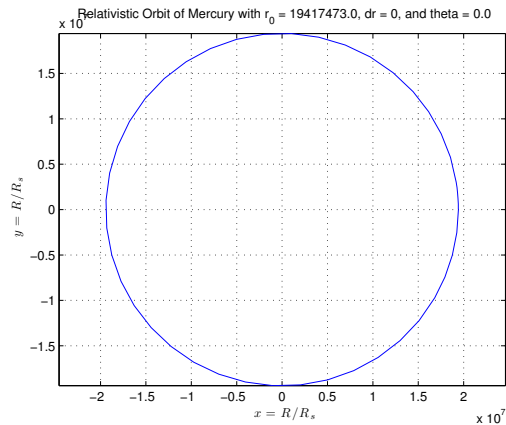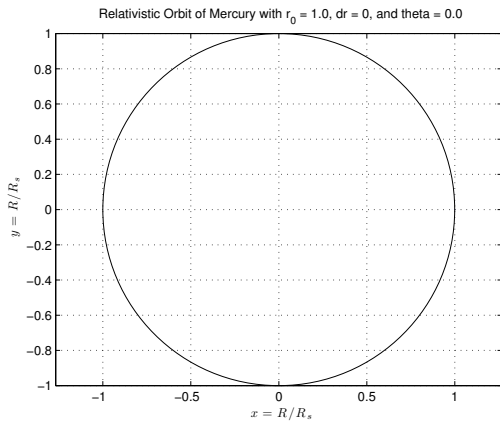

(e) IV More eccentric elliptical orbit

(f) V Hyperbolic orbit

8

Figure 5: The origin for these plots are at (0,0). Caution: Pay attention to axes range before examining plots. The x axis of the plots are for the nondimensionalized parameter $x = \frac{R}{R_s}$ and the y axis is $\frac{dx}{d\tau}$.


(a) Close view of relativistic phase portrait

(b) Far view of relativistic phase portrait

(c) As predicted, if we start at the event horizon (i.e. when $x = \frac{R}{R_s} = 1$), the body wouldn't move. Therefore no orbit is generated. The black circle represents the event horizon.

(d) Plot of the other equilibrium at $x = 1.94 \times 10^7$, which is the same as the average distance between the Mercury and Sun. This equilibrium generates a circular orbit
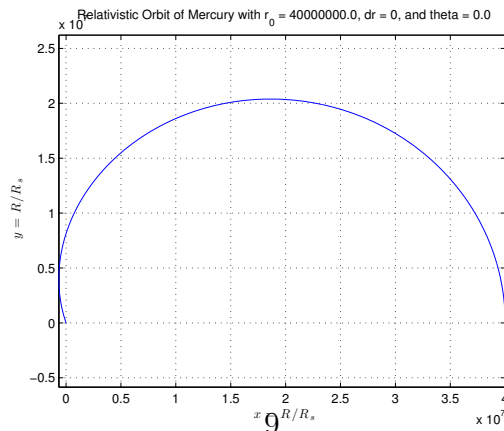
(e) This physical orbit is an example of when the initial conditions are detrimental. Mercury is sent on a collision course towards the origin where it would collide with the Sun.